

Best Practices for Determination of Initial $^{10}\text{Be}/^{9}\text{Be}$ in Early Solar System Materials by Secondary Ion Mass Spectrometry

Emilie T. Dunham , Meenakshi Wadhwa , Steven J. Desch  and Richard L. Hervig 

School of Earth and Space Exploration, Arizona State University, 781 Terrace Mall, Tempe, AZ, 85287, USA

*Corresponding author. e-mail: etdunham@asu.edu

Beryllium-10 ($t_{1/2} = 1.4$ Ma) is a short-lived radionuclide present in the early Solar System. It is produced solely by irradiation reactions and can provide constraints on the astrophysical environment of the Sun's formation. Calcium- and aluminium-rich inclusions (CAIs), the first solids formed in the Solar System, show clear evidence for live ^{10}Be at their time of formation, but it is unclear whether they record the same initial $^{10}\text{Be}/^{9}\text{Be}$ ratio. In this study, we examine the secondary ion mass spectrometry methods used to determine the initial $^{10}\text{Be}/^{9}\text{Be}$ ratio in meteoritic inclusions. Based on analyses of synthesised matrix-matched glass reference materials, we show that the effects of differing major element bulk compositions on the secondary ion yields of Be and B are minor for relevant phases. We demonstrate the importance of using the mean square weighted deviation (MSWD) to interpret the significance of the initial $^{10}\text{Be}/^{9}\text{Be}$ value. For thirty-two CAIs, we re-calculated the regressions using literature data, finding that several have unacceptably high MSWD. We calculate the effects of possible sources of isotopic disturbance. Finally, we outline best practices for reporting ^{10}Be – ^{10}B data, to enable a more refined determination of the initial $^{10}\text{Be}/^{9}\text{Be}$ ratio in the early Solar System.

Keywords: short-lived radionuclides, cosmochemistry, Beryllium-10, SIMS, CAI.

Received 02 Dec 19 – Accepted 10 Apr 20

Beryllium-10, which decays to ^{10}B with a half-life of 1.4 Ma (Korschinek *et al.* 2010), is produced by spallation reactions induced by galactic and/or stellar cosmic rays (McKeegan *et al.* 2000, Desch *et al.* 2004, Liu *et al.* 2010, Tatischeff *et al.* 2014, Jacquet 2019). The former presence of ^{10}Be is inferred by anomalous $^{10}\text{B}/^{11}\text{B}$ ratios (relative to the chondritic value of 0.2481, Zhai *et al.* 1996) in phases with high Be/B ratios (such as melilite) in calcium- and aluminium-rich inclusions (CAIs), the first solids formed in the Solar System. Previous studies over the past two decades have reported ^{10}Be – ^{10}B isotope systematics in many CAIs and have amply demonstrated that live ^{10}Be was present in the early Solar System. However, the inferred initial $^{10}\text{Be}/^{9}\text{Be}$ ratios range from 3×10^{-4} to 1×10^{-2} , even though $\sim 85\%$ of CAIs record initial $^{10}\text{Be}/^{9}\text{Be} \sim (6\text{--}9) \times 10^{-4}$ (McKeegan *et al.* 2000, Sugiura *et al.* 2001, Marhas *et al.* 2002, MacPherson *et al.* 2003, Chaussidon 2006, Liu *et al.* 2010, Wielandt *et al.* 2012, Srinivasan and Chaussidon 2013, Sossi *et al.* 2017, Mishra and Marhas 2019). It is critical to determine whether the distribution of ^{10}Be in the early Solar System was homogeneous or heterogeneous, because that allows us to

infer how it was produced. If ^{10}Be was homogeneously distributed (i.e., CAIs, which likely formed within a narrow time interval, record a single $^{10}\text{Be}/^{9}\text{Be}$ value), it was likely produced by galactic cosmic rays (GCR) interacting with the molecular cloud core that collapsed to form our Solar System (Desch *et al.* 2004, Tatischeff *et al.* 2014). On the other hand, if ^{10}Be was distributed heterogeneously (i.e., CAIs display a range of $^{10}\text{Be}/^{9}\text{Be}$ values), ^{10}Be was likely produced by solar particles interacting with gas and solids in the solar nebula (McKeegan *et al.* 2000, Gounelle *et al.* 2001, MacPherson *et al.* 2003, Jacquet 2019). The origin of ^{10}Be is currently ambiguous partly because of the difficulty of interpreting the results to date.

In order to determine the initial $^{10}\text{Be}/^{9}\text{Be}$ ratios of CAIs, cosmochemists collect Be and B isotopic data via secondary ion mass spectrometry (SIMS) and then perform a York regression on the data to obtain the slopes of the ^{10}Be – ^{10}B isochrons. The ^{10}Be – ^{10}B isotope system is measured by the *in situ* SIMS technique; a primary beam of mass-filtered $^{16}\text{O}^{-}$ ions with high energies (typically 21–23 keV) is directed at a

carefully selected and documented, crack-free, mineral. The cascade of collisions produced by the primary beam in the atoms in the sample results in the ejection of atoms and molecules in a process known as ‘sputtering’; some sputtered material is ionised in the process. A positive potential (typically 5–10 kV) is applied to the sample to accelerate positive secondary ions into a double-focusing mass spectrometer where they are selected for energy and mass. The mass-analysed ion beam is directed to an electron multiplier to record the signal. Because the ionisation probabilities of Be and B are different, the number of counts per second produced for each $\mu\text{g g}^{-1}$ of these elements in a sample is not the same, and comparison with a reference material is needed to calibrate the Be/B ratio.

In the case of a short-lived nuclide such as ^{10}Be , the amount of the daughter isotope (^{10}B) in a sample at the present time that originally contained live ^{10}Be can be expressed as $^{10}\text{B} = ^{10}\text{B}_0 + ^{10}\text{Be}$, where $^{10}\text{B}_0$ and ^{10}Be are the original amounts present in the sample in the early Solar System. Normalisation to a stable isotope of the daughter (^{11}B), then yields the following equation: $^{10}\text{B}/^{11}\text{B} = (^{10}\text{B}/^{11}\text{B})_0 + (^{10}\text{Be}/^{11}\text{B})$. This equation can be re-written as: $^{10}\text{B}/^{11}\text{B} = (^{10}\text{B}/^{11}\text{B})_0 + (^{10}\text{Be}/^9\text{Be}) \times (^9\text{Be}/^{11}\text{B})$. This is the equation for a straight line where the slope and intercept correspond to the initial radioactive parent-to-stable parent ratio ($^{10}\text{Be}/^9\text{Be}$) and the non-radiogenic daughter composition ($^{10}\text{B}/^{11}\text{B}_0$), respectively. Thus, a ^{10}Be – ^{10}B isochron for a CAI is made by plotting the measured $^{10}\text{B}/^{11}\text{B}$ versus $^9\text{Be}/^{11}\text{B}$ ratios for phases in that CAI with varying Be/B ratios, and fitting a straight line through these data points by a least squares regression (Ludwig 1988, Vermeesch 2018). To determine the least squares fit, the York regression method (York 1966, York *et al.* 2004) takes into account independent uncertainties in both the x and y variables and allows for correlations between these uncertainties, to determine the least squares fit.

Therefore, in a ^{10}Be – ^{10}B isochron plot of $^{10}\text{B}/^{11}\text{B}$ versus $^9\text{Be}/^{11}\text{B}$, an age cannot be directly determined, unlike the case for isochron plots for long-lived radioisotope systems, but the slope of the fit represents the inferred initial $^{10}\text{Be}/^9\text{Be}$ ratio, and the intercept is the initial $(^{10}\text{B}/^{11}\text{B})_0$ for that sample. Each of these mean ratios is associated with a standard error, which is typically given as 2SE (95% confidence level for this mean). Statistically, a valid isochron is one that has scatter that can be attributed solely to the measurement errors, such that the reduced chi-squared or mean square weighted deviation (MSWD) is ~ 1 .

When compared with other isotope measurements, there are a number of additional concerns when it comes to

determining ^{10}Be – ^{10}B isotopic systematics. One of the main issues is the typically low mass fractions of Be and B in CAIs. The ^{10}Be – ^{10}B isotope measurements by SIMS are predominantly performed on melilite because when considering the phases commonly found in CAIs, the mineral structure for this phase is best suited to accommodating the small divalent beryllium ion. Moreover, previous studies show a large spread of $^9\text{Be}/^{11}\text{B}$ ratios in this phase. Melilite is a solid solution between $\text{Ca}_2\text{Al}_2\text{SiO}_7$ (gehlenite) and $\text{Ca}_2\text{MgSi}_2\text{O}_7$ (åkemanite). Condensation calculations predict that Be condenses in solid solution with melilite and most likely condenses into Mg and/or Ca sites (Lauretta and Lodders 1997). The Be mass fraction in melilite is usually about 500 ng g^{-1} , while the B mass fraction in melilite varies drastically on $\sim 5 \mu\text{m}$ scales from $\sim 1 \text{ ng g}^{-1}$ to $1 \mu\text{g g}^{-1}$, depending on the sample (MacPherson *et al.* 2003). As described below, uncertainty in the isotope ratios measured by SIMS is particularly sensitive to the denominator species, $^{11}\text{B}^+$. In order to obtain appropriately high intensities of this isotope, it is necessary to increase the amount of the phase being sampled. For example, one sputters the melilite with a large primary ion current (typically 10–30 nA in most IMS-6f and IMS-1270/80 SIMS instruments). This, though, creates a large SIMS pit ($> 20 \mu\text{m}$ diameter), so measuring single grains in fine-grained or small samples is nearly impossible; intersecting multiple melilite crystals and possibly encountering a crack can bias the isotope ratios. Advances in micro-analytical mass spectrometry now allow smaller samples to be analysed, such as with a bright oxygen ion source attached to a SIMS (Liu *et al.* 2018). However, even with a high sputtering rate on a small-diameter crater, $^{11}\text{B}^+$ intensities can be $< 1 \text{ counts s}^{-1}$. Small counts must be treated mathematically with care, to avoid introducing ratio calculation bias, as in the case of ^{60}Fe – ^{60}Ni systematics (Ogliore *et al.* 2011). To avoid such a bias, we use the integrated counts of the two boron isotopes throughout the analysis because the least biased ratio estimation for low count measurements is Beale’s estimator (Telus *et al.* 2013). Other methods to avoid statistical bias when using such low count rates include the Coath method (Coath *et al.* 2013). Regardless of the selected approach, different ratio estimation techniques change the final $^{10}\text{Be}/^9\text{Be}$ value by less than a few per cent. Given the large range in boron isotope ratios and associated high uncertainties observed in CAIs in particular, we suggest the ratio estimation technique approaches are equivalent here.

In addition to these challenges, the ^{10}Be – ^{10}B isotopic system is subject to disturbance. Isotopes of B and Be are otherwise rare and are efficiently produced by irradiation, especially by spallation of O nuclei, which can occur when cosmic rays interact with a meteorite parent body. Adding plausible amounts of extra spallogenic B to CAI melilite can drastically alter the original $^{10}\text{Be}/^9\text{Be}$ signature. Parent body

aqueous alteration can also disturb the ^{10}Be – ^{10}B system by mobilising B; this alteration would likely increase the scatter in a ^{10}Be – ^{10}B isochron for a CAI. These factors intrinsic to the ^{10}Be – ^{10}B isotopic system make it difficult to determine the distribution of ^{10}Be in the early Solar System.

Interpreting the ^{10}Be – ^{10}B data for CAIs in the existing literature is difficult because not all published data sets are complete. Previous ^{10}Be – ^{10}B studies do not always report the necessary information, such as standardisation details and raw data, required to reproduce or interpret the results. Reference materials are necessary to correct for analytical artefacts in SIMS measurement. As an example, matrix-matched reference materials are used to determine the relative sensitivity factor (RSF), which is used to account for the difference in the ionisation of Be with respect to B from a particular matrix. Previous studies have not always reported their RSF, and those that do use a variety of reference materials (most of which do not match the sample matrix), resulting in a range of RSF values (Table 1). For the ^{10}Be – ^{10}B system, suitable matrix-matched reference materials have not been fully developed for phases such as melilite, hibonite ($\text{Ca}(\text{Al,Ti,Mg})_{12}\text{O}_{19}$) or grossite (CaAl_4O_7) with trace mass fractions of Be and B. Moreover, how the major element composition (matrix) of a reference material affects the RSF values for this isotope system is not well understood. Other quantities that tend to not be reported include all the errors needed to reproduce a regression, correlation coefficients and MSWD (or reduced chi-squared) associated with the isochron regressions. Because of the typically low mass fractions of B found in CAI phases, errors in the $^9\text{Be}/^{11}\text{B}$ and $^{10}\text{Be}/^{11}\text{B}$ ratios are correlated; taking the correlation coefficient into account can alter the regression. The MSWD of regressions is necessary to report because this quantity is needed to judge the validity of an isochron.

The purpose of this paper is to establish consistent best practices for measuring and reporting ^{10}Be – ^{10}B data. In doing so, we hope that previous and future studies can be more easily integrated, to elucidate the distribution and origin of ^{10}Be in the early Solar System. We report on melilite glasses we developed to standardise the RSF. We re-evaluate previous ^{10}Be – ^{10}B data to create a unified data set by uniformly constructing the regressions. We discuss factors that can disturb the ^{10}Be – ^{10}B system, such as how irradiation that produces spallogenic B can change the slope of the isochron without affecting the MSWD, and how to assess the effects of irradiation (e.g., using a ^{149}Sm dosimeter). We discuss how aqueous alteration can produce more scatter in the regression, and how to recognise when a CAI has been disturbed by aqueous alteration. Finally, we discuss best practices for reporting regressions, to facilitate

Table 1.
Reference materials for ^{10}Be – ^{10}B measurements

Study	SIMS model	Reference material	RSF
Sugiura <i>et al.</i> (2001)	IMS-6f	JB, JA, JG	2.7
MacPherson <i>et al.</i> (2003)	IMS-6f	NIST SRM 612	2.4–2.7
Chaussidon (2006)	IMS-1270	GB4, BHVO-1, UTR-2	2.5–2.6
Wielandt <i>et al.</i> (2012)	IMS-1280	NIST SRM 612 GSC, GSD	2.6 1.8
Fukuda <i>et al.</i> (2018)	NanoSIMS	Melilite glass NIST SRM 610	2.55 ± 0.11 2.44 ± 0.12
Sossi <i>et al.</i> (2017)	IMS-1280	GB4	3.17 ± 0.13
Mishra and Marhas (2019)	IMS-4f	GB4	2.62–2.95
This study	IMS-6f	NIST SRM USGS GSC-1G, GSD-1G, GSE-1G	2.36 ± 0.13 2.03 ± 0.18
This study	IMS-1290	Melilite glass NIST SRM Melilite glass	2.21 ± 0.18 2.45 ± 0.28 1.91 ± 0.15

comparisons across data sets. The compiled data set from previous literature, in addition to consistent reporting of ^{10}Be – ^{10}B data in future studies, will allow us to constrain the origin of ^{10}Be in the early Solar System.

The role of reference materials in ^{10}Be – ^{10}B isotope measurements

Beryllium is ionised more efficiently than B during SIMS analyses (e.g., Hervig *et al.* 2006), so the Be^+/B^+ ion ratio needs to be corrected for fractionation caused during the sputtering process. To do this, we need to measure reference materials with known Be and B mass fractions (i.e., [Be] and [B], respectively). SIMS measurements of reference materials allow us to calculate a RSF, which is defined as:

$$\text{RSF} = \left(\frac{^9\text{Be}^+}{^{11}\text{B}^+} \right)_{\text{SIMS}} / \left(\frac{^9\text{Be}}{^{11}\text{B}} \right)_{\text{true}} \quad (1)$$

where $(^9\text{Be}^+/\text{B}^+)_{\text{SIMS}}$ is the apparent $^9\text{Be}/^{11}\text{B}$ ion ratio measured via SIMS, and $(^9\text{Be}/^{11}\text{B})_{\text{true}}$ is the actual atomic $^9\text{Be}/^{11}\text{B}$ ratio in a reference material. We then use this RSF to calculate the correct $^9\text{Be}/^{11}\text{B}$ ratio in the sample as follows:

$$\left(\frac{^9\text{Be}}{^{11}\text{B}} \right)_{\text{corrected}} = \left(\frac{^9\text{Be}^+}{^{11}\text{B}^+} \right)_{\text{Uncorrected}} / \text{RSF} \quad (2)$$

In previous studies, the CAI phase most commonly measured for ^{10}Be – ^{10}B isotope systematics is melilite. The RSF for melilite was assumed to be the same as that of the

Table 2.
Elemental and isotopic compositions of relevant reference materials

	GN		G2		GX		NIST SRM 610		NIST SRM 612		NIST SRM 614		USGS GSC-1G		USGS GSD-1G		USGS GSE-1G		GB4
	Mean	2SE	Mean	2SE	Mean	2SE	Mean	2SE	Mean	2SE	Mean	2SE	Mean	2SE	Mean	2SE	Mean	2SE	Mean
Åk mol%	75	–	54	–	20	–	–	–	–	–	–	–	–	–	–	–	–	–	–
SiO ₂ (% m/m)	37.1	0.4	37.2	1.1	25.5	0.6	69.7	0.5	72.1	0.6	72.1	0.9	52.6	0.6	53.2	0.8	53.7	1.5	72.9
MgO (% m/m)	10.7	0.3	7.9	0.3	2.6	0.4	–	–	–	–	–	–	3.6	0.0	3.6	0.0	3.5	0.0	–
Al ₂ O ₃ (% m/m)	7.3	0.1	20.6	0.7	27.2	0.5	2.0	0.1	2.0	0.1	2.0	0.1	13.5	0.4	13.4	0.3	13.0	0.4	15.6
CaO (% m/m)	44.7	0.3	34.1	1.0	44.5	0.8	11.4	0.2	11.9	0.1	11.9	0.2	7.1	0.1	7.2	0.1	7.4	0.3	0.6
Na ₂ O (% m/m)	0.1	0.1	0.2	0.1	0.1	0.1	13.4	0.3	13.7	0.3	13.7	0.3	3.6	0.2	3.6	0.3	3.9	0.2	4.6
Be (µg g ⁻¹)	554.8	25.5	567.7	26.1	630.9	29	476	31	37.5	1.5	0.8	0.1	4.5	0.4	46	5	490	80	11.3
B (µg g ⁻¹)	15.6	1.6	48.3	5.8	85	8.8	350	56	34.3	1.7	1.5	0.2	26.0	7.0	50	20	330	120	970
⁹ Be/ ¹¹ B	53.2	5.9	19.5	2.5	10	1.1	2.17	0.37	1.7	0.1	0.8	0.1	0.26	0.07	1.38	0.57	2.23	0.89	–
IMS-6f																			
⁹ Be ⁺ / ¹¹ B ⁺	116.78	4.22	43.36	2.79	22.37	2.97	4.87	0.07	4.05	0.07	2.26	0.17	0.54	0.01	2.39	0.02	3.87	0.02	–
δf RSF	2.19	0.25	2.22	0.32	2.24	0.39	2.25	0.39	2.32	0.15	2.80	0.45	2.09	0.59	1.73	0.72	1.74	0.69	–
IMS-1290																			
⁹ Be ⁺ / ¹¹ B ⁺	97.34	4.34	36.73	5.38	20.37	1.29	4.63	0.02	–	–	2.32	0.04	–	–	–	–	–	–	–
1290 RSF	1.82	0.22	1.88	0.37	2.04	0.26	2.14	0.37	–	–	2.89	0.43	–	–	–	–	–	–	–

The melilite-composition glasses synthesised here, GN, G2 and GX, are representative of the range of Åk composition found in CAs. The elemental data for the other reference materials are from the literature (NIST SRM 610, 612, 614: Jochum *et al.* 2011; USGS GSC-1G, USGS GSD-1G, USGS GSE-1G: Jochum *et al.* 2005, GB4: Chaussidon 2006).

commonly available silicate glasses (Table 1), which have RSF values of ~ 2.5–3.2 depending on the study and the specific reference material measured. Changes in ionisation probabilities as a function of major element mass fraction have often been observed in SIMS analyses (Ihinger *et al.* 1994, Ottolini *et al.* 2002), so it is preferable that reference materials have a bulk composition similar to the unknown sample (i.e., are matrix-matched). However, the chemical compositions of these glass reference materials are very different from melilite (Table 2).

The consequence of using an RSF from an inappropriate reference material is that the resulting inferred ¹⁰Be/⁹Be ratios for CAs could be underestimated or overestimated. Fukuda *et al.* (2018) synthesised melilite-composition glasses containing trace amounts of Be and B to test if the RSF was different than silica-rich glasses. They used the University of Tokyo NanoSIMS to determine that the RSF is the same between melilite-composition glass and the reference material NIST SRM 610. As described in section *Synthesising melilite-composition glasses*, we have also synthesised melilite-composition glasses and determined the RSF on two other SIMS instruments: SIMS IMS-6f at Arizona State University (ASU) and IMS-1290 at University of California, Los Angeles (UCLA).

The ¹⁰B/¹¹B ion ratio determined on the sample must also be corrected for instrumental mass fractionation (IMF), which occurs during the process of sputtering, transmission through the mass spectrometer, and detection. In general, the ¹⁰B/¹¹B ratio is higher than bulk-analysed (‘true’) values because all boron ions have the same kinetic energy, but the lighter isotope has higher velocity, possibly allowing it to avoid neutralising collisions as it leaves the sample surface. The velocity effect has been studied in detail for B and other isotopic systems (Gnaser and Hutcheon 1987). This will only play a role in the measured isotope ratio if: (a) the energy bandpass is small (unlikely for most SIMS analyses); and (b) sample charging is not controlled. Another cause of uncertainty in correcting the raw ¹⁰B⁺/¹¹B⁺ ion ratio to true atomic ratios is the effect of changing bulk chemistry. While some studies (e.g., Sugiura *et al.* 2001, Marschall and Monteleone 2014) suggest that bulk chemistry does not have a significant effect on fractionation of boron isotopes during sputtering, Rosner *et al.* (2008) found a ~ 3‰ effect between NIST SRM 610 and NIST SRM 612 synthetic glasses relative to natural silicate glasses with a wide range of chemistry. In a follow-up study, De Hoog *et al.* (2017) found that hydrous minerals showed different IMF for boron isotopes than natural glasses by a few permil. However, because the

boron isotope ratios measured in CAI phases typically vary by a factor of nearly 2, any matrix effects on the IMF correction for their boron isotope compositions are relatively minor compared with the typical analytical errors and we can safely use the synthetic NIST SRM glass reference materials to correct for this fractionation. The IMF is calculated as follows:

$$\text{IMF} = \left(\frac{{}^{10}\text{B}^+}{{}^{11}\text{B}^+} \right)_{\text{SIMS}} / \left(\frac{{}^{10}\text{B}}{{}^{11}\text{B}} \right)_{\text{true}} \quad (3)$$

The measured B isotope ion ratio is normalised to the value of the IMF to generate the corrected B isotope ratio. Typical values of IMF for our analyses vary from ~ 1.02 to 1.04.

Synthesising melilite-composition glasses

Glasses of melilite composition doped with Be and B were synthesised at ASU. In ASU's Isotope Cosmochemistry and Geochronology Lab (a class 1000 clean laboratory), 99.9% or higher purity Alfa Aesar oxide powders of MgO, CaCO₃, SiO₂ and Al₂O₃ were weighed in different proportions (total ~ 4 g for each glass) to produce three melilite-composition powders with varying åkermanite content, and each of these powders was doped with different amounts of BeO (American Beryllia) and B(OH)₃ (NIST SRM 951 boric acid) using a microbalance. Each powder was then mixed in a mortar and pestle with methanol for at least 10 min. These mixtures were subsequently converted to glasses in the Depths of the Earth laboratory at ASU. A 50 ml volume Pt crucible was filled with the powder mixture and lowered into a DelTech furnace, the temperature raised to 1050 °C at 3 °C min⁻¹ in order to allow the CO₂ to release slowly and then to 1600 °C at 10 °C min⁻¹. After 3 h at this liquidus temperature, the crucible was dropped into water for rapid quenching. This glass was removed from the crucible, ground to a powder by mortar and pestle, and the melting process repeated at least two times to ensure homogenisation.

Elemental compositions of melilite-composition glasses

Glass fragments from the synthesised melilite-composition glasses (section above) were co-mounted in epoxy (EpoxySet resin and hardener from Allied) and polished. Major elements were determined using the JEOL JXA-8530F electron probe microanalyser (EPMA). For the EPMA, we used 15 kV accelerating voltage and an electron current of 15 nA and obtained thirteen or more energy dispersive spectra of MgO, Al₂O₃, SiO₂ and CaO abundances per sample.

The Be and B contents of the three synthesised glasses (GN, G2 and GX) were measured using the iCAP-Q quadrupole inductively coupled plasma-mass spectrometer (ICP-MS) at ASU. For each of the three synthetic glasses, we started with four powdered 15–50 mg aliquots. To measure the B content, following the procedure of Gangjian *et al.* (2013), two of the four powdered aliquots for each glass were mixed in a PTFE container with 1 ml concentrated HF, 100 µl H₂O₂, and 100 µl 1% mannitol solution and were digested by heating on a hot plate at 60 °C for 3 days. These aliquots were ultimately brought into 3% nitric solution, and their B mass fractions were measured using the standard addition technique on the iCAP-Q ICP-MS. To measure Be, we digested the other two powdered aliquots for each glass in 2 ml concentrated nitric and 0.4 ml concentrated HF at 80 °C for a day. Following digestion and drying down, each residue was brought into solution with 5 ml 6 mol l⁻¹ HCl. The dry down and treatment with HCl was repeated to ensure complete dissolution. After drying down a final time, each residue was brought into final solution with 1.2 ml of 3% nitric prior to analyses with the iCAP-Q ICP-MS. The GN, G2 and GX solutions were measured against six standard solutions with a range of B and Be contents from 0 to 155 µg g⁻¹. The elemental compositions of the melilite-composition synthetic glasses are shown in Table 2.

SIMS investigations of melilite-composition glasses

We conducted measurements of ¹⁰Be/¹⁰B ratios on the synthesised melilite-composition glasses (GN, G2 and GX) using the Cameca IMS-6f SIMS at ASU and the Cameca IMS-1290 SIMS at the UCLA. We measured the glasses on both instruments to test for any variation in RSF on different instruments (Tables 1 and 2). The results shown in Tables 1 and 2 for these glasses are based on means of three or more analyses for each glass composition. These tables also show data based on reference materials analysed by previous studies. We note that some previous studies do not report the RSF value but do report the reference material(s) that they used. For example, McKeegan *et al.* (2000) used GB4, a high-silica natural sample melted and quenched to a glass; Srinivasan and Chaussidon (2013) used a set of in-house and well-known reference glasses (basaltic, pyroxene and melilite composition, as well as BHVO and NBS); Liu *et al.* (2010) used NIST SRM 612.

Analyses with Cameca IMS-6f SIMS (Arizona State University)

The Cameca duoplasmatron was used to generate the primary ion beam, and samples were held at a potential of

12.5 kV. Using a current of ~ 10 nA, the $^{16}\text{O}^-$ primary beam was focused to a spot ~ 20 μm in diameter. No energy filtering was applied. We operated the mass spectrometer at a mass resolving power (MRP) of ~ 1500 to resolve and avoid interferences on ^9Be (from $^{27}\text{Al}^{3+}$) as well as ^{10}B and ^{11}B from ^9BeH and ^{10}BH interferences (other interferences such as $^{30}\text{Si}^{2+}$ are also separated at these conditions). We caution that calibrating the SIMS with MRP greater than ~ 1200 is necessary to resolve ^9BeH from ^{10}B to obtain accurate results, and high-resolution mass scans should be conducted to ensure that the interference is resolved. For the melilite-composition glasses, we measured ^9Be (8 s), ^{10}B (16 s) and ^{11}B (4 s) during thirty cycles for each measurement. At the end of each analysis, ^{28}Si was additionally measured as a reference. The $\text{M}^+ / ^{28}\text{Si}^+$ ion ratios (after normalising to the known SiO_2 content of the reference materials) were used to determine calibration factors for calculating the Be and B contents of the unknown materials. The RSF values from this study are reported in Table 1 as weighted means of the analyses of different reference materials ('NIST' is a weighted mean of analyses of NIST SRM 610, 612 and 614 glasses; 'GSC, GSD, GSE' is a weighted mean of analyses of USGS GSC-1G, USGS GSD-1G and USGS GSE-1G glasses; 'Melilite glass' is a weighted mean of the analyses of the three synthesised glasses). Table 2 provides the individually determined RSF values for the different glass reference materials (the three synthesised melilite-composition glasses, the NIST SRM 610, 612 and 614 glasses, and the USGS GSC-1G, USGS GSD-1G and USGS GSE-1G glasses).

Analyses with Cameca IMS-1290 SIMS (University of California, Los Angeles)

A 5–10 nA $^{16}\text{O}^-$ primary beam resulting in a beam diameter ~ 5–10 μm was generated by a *Hyperion-II* RF source (Liu *et al.* 2018). The mass resolving power was ~ 2500, the entrance and exit slits were fully open, the aperture was 750 μm , and the image field was 80 μm . Secondary ion intensities were measured in peak jumping mode with three electron multipliers (EM). The first mass jump with a 5 s count time measured $^{27}\text{Al}^{3+}$ and $^{28}\text{Si}^{3+}$, the second mass jump with a 10 s count time measured $^9\text{Be}^+$ and the third mass jump with a 40 s count time measured $^{10}\text{B}^+$ and $^{11}\text{B}^+$. Pre-sputtering (without raster) for 3 min was used to remove surface B contamination. The RSF values from this study are reported in Table 1 as weighted means of the analyses of different reference materials ('NIST' is a weighted mean of analyses of NIST SRM 610 and 614 glasses; 'Melilite glass' is a weighted mean of the analyses the three synthesised glasses). Table 2 provides the individually determined RSF values for the different glass reference

materials (the three synthesised melilite-composition glasses, and the NIST SRM 610 and 614 glasses).

Determining RSF with matrix-matched SIMS reference materials

In SIMS analyses, the correct value of the RSF based on the measurement of appropriate reference materials must be used for determining accurate ^{10}Be – ^{10}B isotope systematics. To illustrate this, we created two example isochrons with data and associated (2SE) errors comparable to a real CAI isochron (Figure 1). When $\text{RSF} = 2$, initial $^{10}\text{Be}/^9\text{Be} = (6.0 \pm 1.2) \times 10^{-4}$, while when $\text{RSF} = 3$, initial $^{10}\text{Be}/^9\text{Be} = (9.0 \pm 1.8) \times 10^{-4}$. In both cases, $\text{MSWD} = 1$. Importantly, the $^9\text{Be}/^{11}\text{B}$ ratio and the uncertainties in this ratio are both inversely proportional to the RSF multiplied by the ^9Be counts and divided by the ^{11}B counts, so that MSWD is not affected by the RSF. As can be seen here, when the RSF is increased by ~ 50%, the inferred initial $^{10}\text{Be}/^9\text{Be}$ ratio correspondingly increases by ~ 50%. However, given the relatively large uncertainties, the $^{10}\text{Be}/^9\text{Be}$ values are just within uncertainty of each other. This exercise shows that it is important to evaluate matrix effects and determine the best reference material(s) to obtain the most accurate SIMS data for constraining ^{10}Be – ^{10}B isotope systematics. Nevertheless, because of the typically large uncertainties involved in such measurements, using an imperfect reference material may not significantly alter the results.

Indeed, due to the intrinsically large uncertainties when measuring trace amounts of Be and B in CAIs, we show here that the use of a matrix-matched reference material (i.e., composition of the reference material is similar to the composition of the unknown sample) may not be critical. Like Fukuda *et al.* (2018), we synthesised and measured matrix-matched melilite-composition glass. However, we used different synthesis techniques and determined the RSF using an IMS-6f and an IMS-1290 SIMS to validate the results from the Fukuda *et al.* (2018) NanoSIMS study. We find that, in general, matrix-matched reference materials may not be critical for accurate ^{10}Be – ^{10}B isotopic measurements. This is broadly in agreement with the results reported by Fukuda *et al.* (2018). Our IMS-6f SIMS data (Tables 1, 2; Figure 2a) show that the NIST SRM glasses 610, 612 and 614 ($\text{SiO}_2 = 70\%$ m/m , $[\text{B}] = 0.8\text{--}476.0 \mu\text{g g}^{-1}$) define a weighted mean $\text{RSF} = 2.36 \pm 0.13$ while our melilite-composition glasses ($\text{SiO}_2 \sim 25\text{--}38\%$ m/m , $[\text{B}] = 16\text{--}85 \mu\text{g g}^{-1}$, $[\text{Be}] \sim 600 \mu\text{g g}^{-1}$) with varying \AA k content ($\text{\AA k}_{20\text{--}75}$), GX, G2 and GN, define a weighted mean $\text{RSF} = 2.21 \pm 0.18$. However, our IMS-1290 SIMS data (Tables 1, 2; Figure 2b) are more complex. While one of the NIST SRM glasses (610) defines the same RSF (2.14 ± 0.37) as the melilite-

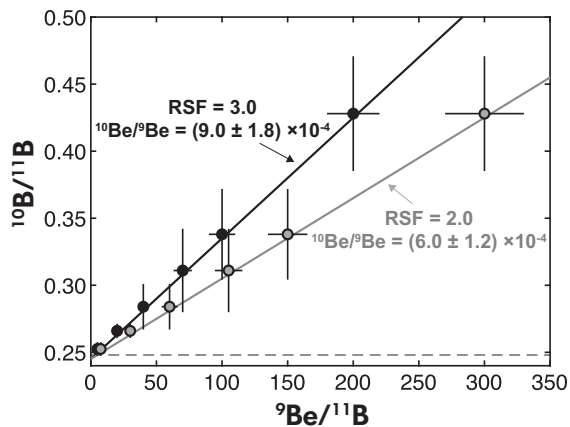


Figure 1. An example of a ^{10}Be – ^{10}B isochron (based on hypothetical data, with 2SE errors, comparable to those reported in the previous literature for CAIs), demonstrating the effect of RSF on the $^{10}\text{Be}/^9\text{Be}$ slope. Using different RSF values changes the slope without altering the MSWD. The horizontal dashed line is the chondritic B isotope ratio ($^{10}\text{B}/^{11}\text{B} = 0.2481$; Zhai *et al.* 1996). Because the regressions are hypothetical, they both have MSWD = 1.

composition glasses (1.91 ± 0.15) within the uncertainties, the other NIST SRM glass (614) defines a resolvably higher RSF (2.89 ± 0.43) than the melilite-composition glasses. The reason for the slight difference noted here between the RSFs determined using the IMS-6f and IMS-1290 SIMS instruments is not well understood, but could potentially be related to different instrument characteristics, such as mono-collection versus multi-collection, respectively, or differences in electron multiplier gain settings.

Because at present it is not clear why some reference materials yield somewhat different RSF values than the melilite-composition glasses, it is suggested that homogeneous matrix-matched reference materials (containing Be and B mass fractions comparable to those in CAIs) should be utilised where possible in determining ^{10}Be – ^{10}B isotope systematics of CAIs. It would be beneficial to measure the true Be and B mass fractions of the melilite-composition glasses with higher precision to better understand the intricacies of standardisation for determining ^{10}Be – ^{10}B isotope systematics.

Re-evaluation of literature data

York regression calculation and isochron validity

To calculate a York regression (implemented using IsoplotR; Vermeesch 2018) to determine the $^{10}\text{Be}/^9\text{Be}$ ratio,

the required inputs are as follows: $x = ^9\text{Be}/^{11}\text{B}$; σ_x , the \pm 2SE uncertainty in x ; $y = ^{10}\text{B}/^{11}\text{B}$; σ_y , the \pm 2SE uncertainty in y ; and r , the correlation coefficient of the x and y uncertainties. These inputs are supplied for multiple data points indexed by i , from 1 to N . The outputs of the York regression are the slope (i.e., the $^{10}\text{Be}/^9\text{Be}$ ratio), the \pm 2SE uncertainty in this slope, the intercept (the initial $^{10}\text{B}/^{11}\text{B}$ ratio), the \pm 2SE uncertainty in this intercept, and MSWD.

The correlation coefficient, r , is a common way to measure the credibility of a linear relationship between two variables. Values lie between -1 and 1, with a 1 indicating a perfect positive correlation, -1 indicating a perfect anticorrelation and 0 indicating no correlation. In this context, however, the correlation coefficient is an input provided at each data point i . It is given by:

$$r_i = \frac{\sigma_{xy}^2}{\sigma_x \sigma_y} \quad (4)$$

where σ_x and σ_y are the standard deviations in x and y , and σ_{xy} is the covariance. This is not formally defined if the data point i corresponds to a single measurement, but in the case of ^{10}Be – ^{10}B isotope systematics, multiple cycle counts are combined to provide x , σ_x , y , σ_y and r . If x and y are measured in N_{cycles} cycles corresponding to a single analysis spot (or data point), then

$$\sigma_x^2 = \frac{1}{N_{\text{cycles}}} \sum |x - \mu_x|^2 \quad (5)$$

$$\sigma_y^2 = \frac{1}{N_{\text{cycles}}} \sum |y - \mu_y|^2 \quad (6)$$

$$\text{and } \sigma_{xy}^2 = \frac{1}{N_{\text{cycles}}} \sum (x - \mu_x)(y - \mu_y) \quad (7)$$

where $\mu_x = (1/N_{\text{cycles}}) \sum x$ and $\mu_y = (1/N_{\text{cycles}}) \sum y$ are the mean values, which are reported as x_i and y_i . Because both $x_i = (^9\text{Be})/(^{11}\text{B})$ and $y_i = (^{10}\text{B})/(^{11}\text{B})$ have ^{11}B in the denominator, the uncertainties in x and y are correlated. The low mass fraction of ^{11}B often means it is the dominant source of measurement error, which can make the correlation stronger (i.e., the high $^9\text{Be}/^{11}\text{B}$ analyses often have r values closer to 1). The assumption that x_i and y_i are uncorrelated overestimates the inherent uncertainty in the data and allows a broader range of slopes within the uncertainty envelope for the regression; as such, r should be used for the most accurate and precise determination of ^{10}Be – ^{10}B isotope systematics.

The MSWD value is used to assess the degree of over- or under-dispersion of the data and is particularly important

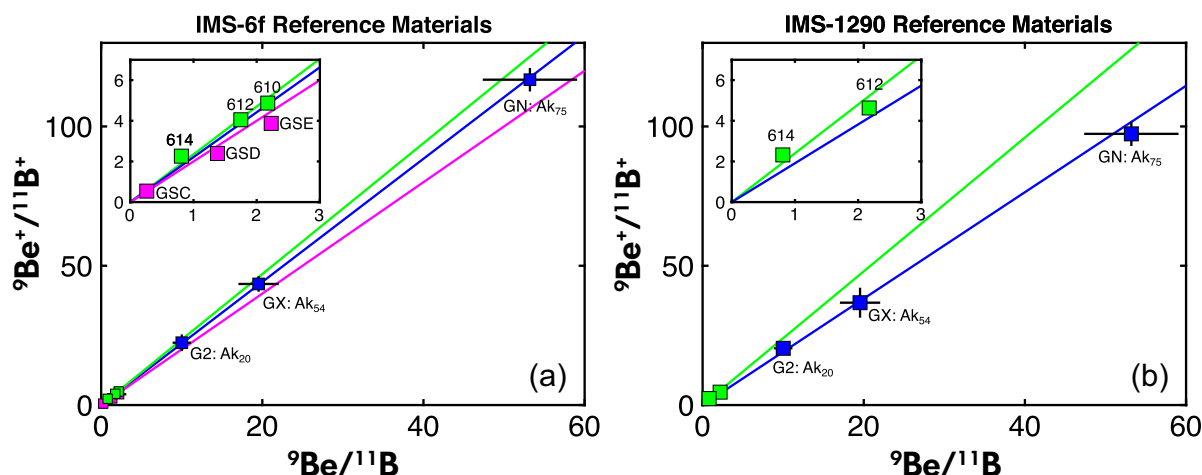


Figure 2. Relative sensitivity factors (RSF) of NIST SRM 610, 612 and 614 (green symbols; Jochum *et al.* 2011), USGS GSC-1G, USGS GSD-1G and USGS GSE-1G (magenta symbols; Jochum *et al.* 2005), and melilite-composition glasses G2, GX and GN (blue symbols; this study) utilising the IMS-6f (a) and the IMS-1290 (b). The RSFs are based on the slopes of ${}^9\text{Be}^+ / {}^{11}\text{B}^+$ (measured by SIMS) vs. ${}^9\text{Be} / {}^{11}\text{B}$ (true atomic ratios, literature values for the reference materials and values for the melilite glasses measured independently in this study by ICP-MS) for these reference materials. Uncertainties are 2SE.

when an isochron has few data points. This value is calculated using the equation:

$$\text{MSWD} = \frac{1}{N-2} \sum_{i=1}^N \frac{(y_i - a - bx_i)^2}{\sigma_{y_i}^2 + b^2 \sigma_{x_i}^2} \quad (8)$$

where a is the inferred intercept of the fit and b is the inferred slope, N is the number of data points in the fit, and x_i and y_i are ${}^9\text{Be} / {}^{11}\text{B}$ and ${}^{10}\text{B} / {}^{11}\text{B}$ values in our case. To determine the significance of the linear fit, we also calculate the uncertainty of the MSWD. For a data set with two terms (in this case, ${}^9\text{Be} / {}^{11}\text{B}$ and ${}^{10}\text{B} / {}^{11}\text{B}$), the expected value of the MSWD is $1 \pm 2\sigma_{\text{MSWD}}$, where as follows:

$$\sigma_{\text{MSWD}} = \sqrt{\frac{2}{(N-2)}} \quad (9)$$

For example, in a ${}^{10}\text{Be} - {}^{10}\text{B}$ isotope data set with 20 x - y pairs that defines a good isochron, the MSWD should be 1.0 within ± 0.67 (at $2\sigma_{\text{MSWD}}$), that is, MSWD should not exceed 1.67. If the fit yields an MSWD higher than this 2-sigma limit, there is a less than $\sim 5\%$ probability that the data conform to a simple linear model, and scientific inferences based on that model are statistically inappropriate. In other words, the linear regression to the data with too-high MSWD has $< 5\%$ probability of being a line and should not be considered an isochron (Wendt and Carl 1991). In such cases for the ${}^{10}\text{Be} - {}^{10}\text{B}$ system, the SLR ${}^{10}\text{Be}$ may have been present in that

CAI, but the slope of the isochron, that is, the inferred initial ${}^{10}\text{Be} / {}^9\text{Be}$ ratio, is too uncertain to report.

Correlation coefficient of the uncertainties in ${}^9\text{Be} / {}^{11}\text{B}$ and ${}^{10}\text{B} / {}^{11}\text{B}$

Few previous studies (MacPherson *et al.* 2003, Wielandt *et al.* 2012) have taken into account the correlation coefficient of the uncertainties in ${}^9\text{Be} / {}^{11}\text{B}$ and ${}^{10}\text{B} / {}^{11}\text{B}$ on the inferred ${}^{10}\text{Be} / {}^9\text{Be}$ ratios. Because raw cycle-by-cycle data are necessary to calculate this correlation coefficient, r , we cannot determine this for previously reported analyses where such data are not provided. This correlated component of the uncertainties in the measured data should be reported in future ${}^{10}\text{Be} - {}^{10}\text{B}$ studies.

In estimating this correlation coefficient for previously published data, we find that the data points with higher ${}^9\text{Be} / {}^{11}\text{B}$ and ${}^{10}\text{B} / {}^{11}\text{B}$ ratios tend to have a higher correlation coefficient. Overall, the inferred initial ${}^{10}\text{Be} / {}^9\text{Be}$ and initial ${}^{10}\text{B} / {}^{11}\text{B}$ ratios do not change significantly. However, the uncertainty associated with the inferred ${}^{10}\text{Be} / {}^9\text{Be}$ ratio generally decreases when the correlation in the uncertainties in ${}^9\text{Be} / {}^{11}\text{B}$ and ${}^{10}\text{B} / {}^{11}\text{B}$ are taken into account, in agreement with MacPherson *et al.* (2003). For example, we found a CAI (Dunham *et al.* 2017) to have initial ${}^{10}\text{Be} / {}^9\text{Be} = (6.8 \pm 2.8) \times 10^{-4}$ (MSWD = 0.5) when correlated errors were not taken into account and

$^{10}\text{Be}/^{9}\text{Be} = (6.7 \pm 2.2) \times 10^{-4}$ (MSWD = 0.6) when correlated errors were included in the York regression. As can be seen in this case, the uncertainty in the inferred initial $^{10}\text{Be}/^{9}\text{Be}$ changes more significantly than the $^{10}\text{Be}/^{9}\text{Be}$ value itself; the MSWD can also change slightly when correlated errors are taken into account. Although the correlation coefficient in the uncertainties in $^{9}\text{Be}/^{11}\text{B}$ and $^{10}\text{B}/^{11}\text{B}$ is not the most important factor in determining the robustness and accuracy of an inferred initial $^{10}\text{Be}/^{9}\text{Be}$ ratio, this parameter should be considered and reported to produce the most complete ^{10}Be – ^{10}B data set.

Re-calculating ^{10}Be – ^{10}B isotope systematics from previous studies

Previous ^{10}Be – ^{10}B studies present data in different ways, and sometimes do not include key components, such as MSWD, so an important goal in this study was to re-calculate all previously reported data using a consistent method to create a single combined data set. We did this by first gathering the reported SIMS data (i.e., $^{9}\text{Be}/^{11}\text{B}$ and $^{10}\text{B}/^{11}\text{B}$ ratios) for thirty-two CAI samples from the previous literature (McKeegan *et al.* 2000, Sugiura *et al.* 2001, Marhas *et al.* 2002, MacPherson *et al.* 2003, Chaussidon 2006, Liu *et al.* 2010, Wielandt *et al.* 2012, Srinivasan and Chaussidon 2013, Sossi *et al.* 2017, Mishra and Marhas 2019). The $^{9}\text{Be}/^{11}\text{B}$ ratios that we extracted from literature were calculated by the authors using comparable RSF values. We entered these data into IsoplotR (Vermeesch 2018) for each CAI to produce an isochron and recorded the results (Table 3). In each case, we evaluated the robustness of the isochron by reporting the MSWD as well as the $1 + 2\sigma_{\text{MSWD}}$; if the MSWD $> 1 + 2\sigma_{\text{MSWD}}$, the regression must be considered in detail to evaluate its validity.

Examining the re-calculated data set

Our re-calculated data set (Table 3) shows that seven out of thirty-two regressions have MSWD $> 1 + 2\sigma_{\text{MSWD}}$. We will not discuss the individual regressions in detail but note that regressions with high MSWD tend to come from CAIs in CH/CB chondrites, or from fine-grained CAIs (Gounelle *et al.* 2013, Sossi *et al.* 2017).

Two CAI regressions have exceptionally high inferred initial $^{10}\text{Be}/^{9}\text{Be}$ ratios when compared with other CAIs (Gounelle *et al.* 2013, Sossi *et al.* 2017), and both are associated with high MSWD. This indicates that the high $^{10}\text{Be}/^{9}\text{Be}$ ratios are inferred from invalid isochrons; the CAIs likely contained live ^{10}Be , but the inferred $^{10}\text{Be}/^{9}\text{Be}$ ratios are unreliable. One of these regressions with high inferred $^{10}\text{Be}/^{9}\text{Be}$ and high MSWD includes a multi-CAI regression

(three fine-grained CAIs; Sossi *et al.* 2017). We argue that fine-grained CAIs should be treated with caution when determining ^{10}Be – ^{10}B systematics. If a SIMS spot covers more than a single, crack-free, melilite grain, it is probable that the isotope determinations will be inaccurate.

Evidence for irradiation

Even after checking that the SIMS analyses are conducted on clean, crack-free areas of pristine (i.e., no evidence of aqueous alteration) CAIs, and selecting only regressions with acceptable MSWD values, the inferred $^{10}\text{Be}/^{9}\text{Be}$ ratios still may not represent the original $^{10}\text{Be}/^{9}\text{Be}$ ratios at the time the CAI formed. In fact, irradiation can artificially elevate the inferred initial $^{10}\text{Be}/^{9}\text{Be}$ ratio. In the top 1–2 m of parent body regolith, energetic ions such as GCRs can irradiate heavy nuclei, such as O, Mg, or Si, to generate light nuclei. Or, secondary protons and neutrons generated by this process can spall nuclei. Because the concentration of secondary protons and neutrons generated depends on the types of nuclei in the meteorite, the production rates of Be and B depend on the parent body composition, and are uncertain to within ~ 50% (Leya *et al.* 2000). For the GCR fluences ($\sim 10^{14}$ – 10^{15} cm $^{-2}$) typically experienced by meteorites within a few metres of their parent body's surface, ng g $^{-1}$ changes in the mass fractions of Be and B can be generated. Typically, the spallogenic $^{10}\text{B}/^{11}\text{B}$ ratio is ~ 0.44, significantly higher than the chondritic ratio $^{10}\text{B}/^{11}\text{B} \sim 0.2481$ (Zhai *et al.* 1996, Liu *et al.* 2010). Because B mass fractions are sometimes as low as a few ng g $^{-1}$ in CAIs, this spallogenic component cannot always be neglected.

Addition of spallogenic B to a CAI would lower the $^{9}\text{Be}/^{11}\text{B}$ ratios and raise the $^{10}\text{B}/^{11}\text{B}$ ratios, both effects tending to artificially increase the slope, steepening the isochron. Addition of spallogenic Be would have the opposite effect, but in general its effect on the total Be mass fraction is comparatively negligible because Be contents are much higher than B contents in melilite (typically, [Be] ~ 500 $\mu\text{g g}^{-1}$ and [B] ~ 10 ng g $^{-1}$). To approximate Be and B production by irradiation, we consider an oxygen target because it has a significantly higher abundance than nitrogen or carbon in CAIs and the reactions to produce Be and B from O are efficient. Using the cross sections for spallation of ^{16}O by high-energy protons ($^{16}\text{O}(\text{p},\text{x})^{11}\text{B} \sim 25$ mbarn while $^{16}\text{O}(\text{p},\text{x})^{10}\text{Be} \sim 2$ mbarn; Moskalenko and Mashnik 2003), we estimate the ratio of spallogenic Be to spallogenic B ($\Delta[\text{Be}]/\Delta[\text{B}]$) of ~ 0.1. It might be expected that addition of spallogenic Be or B might also increase the scatter in the data and the MSWD, but in fact the isochron is not automatically worsened by irradiation.

Table 3.
Compiled $^{10}\text{Be} - ^{10}\text{B}$ data set from previous studies

Meteorite	Chondrite type	CAI sample	CAI-type	[B] range ¹	[Be] range ¹	Initial $^{10}\text{Be}/^{9}\text{Be}^m$	2SE	Initial $^{10}\text{Be}/^{9}\text{Be}^n$	2SE	$^{10}\text{B}/^{11}\text{B}$	2SE	n	MSWD	$1 + 2\sigma_{\text{MSWD}}$	Validity ^P
Isheyevo ^a	CH/CB	501, 503, 2006, 2012	hib-gros-px-mel-sp	13-214		13.1	4.3	13.5	7.4	0.2492	0.0005	13	0.7	1.8	YES
Isheyevo ^a	CH/CB	Isheyevo	hib-gros-px-mel-sp	6-300		104.0	16.0	103.9	31.3	0.2537	0.0033	4	4.5	2.6	NO
Murchison ^b	CM2	Many PLACS	PLAC			5.2	2.8	5.2	2.6	0.2723	0.0160	9	1.4	2.0	YES
Murchison ^c	CM2	Many PLACS	PLAC	1-1526	14-819	5.5	2.6	5.3	1.0	0.2513	0.0013	23	1.1	1.6	YES
Axtell ^d	CV3ox	AXCAI 2771	FUN A	1-10	56-400	3.0	1.2	3.0	1.2	0.2470	0.0220	6	5.2	2.3	NO
Axtell ^e	CV3ox	AXCAI 2771	FUN A	1-11	54-464	2.8	0.2	4.0	0.4	0.2518	0.0036	10	1.1	1.9	YES
NWA 779 ^e	CV3ox	KTI 3898	FUN A	1-63	25-1214	3.4	0.2	5.0	0.4	0.2543	0.0032	12	0.9	1.9	YES
Allende ^d	CV3ox	1	CTA	5-156	120-790	4.8	1.7	4.8	1.7	0.2573	0.0080	7	0.3	2.2	YES
Allende ^f	CV3ox	2	B	4-23		5.3	2.4	5.5	2.6	0.2550	0.0280	7	1.0	2.2	YES
Allende ^f	CV3ox	2	B	7-695		6.9	0.5	7.0	1.1	0.2513	0.0019	12	1.5	1.9	YES
Allende, NWA8616 ^{g*}	CV3ox	2 coarse-grained	B	< 10-80	< 10-40	12.0	3.0	9.3	0.8	0.2488	0.0006	20	8.2	1.6	NO
Allende ^h	CV3ox	3529-41	B	6-927		9.5	1.9	9.8	2.2	0.2540	0.0007	10	0.4	1.9	YES
Allende ⁱ	CV3ox	3529-41	B	10-300		8.8	0.6	10.0	0.9	0.2549	0.0004	51	12.0	1.4	NO
Allende ^{g*}	CV3ox	3 fine-grained	FTA	70-910	< 10-30	71.0	24.0	54.5	9.4	0.2472	0.0007	19	4.4	1.7	NO
Vigarano ^d	CV3red	477-4b	B1	2-85	120-450	5.3	1.7	5.3	1.7	0.2444	0.0022	13	1.0	1.8	YES
Efremovka ^f	CV3red	E38	B	4-106		6.0	1.2	5.7	1.2	0.2550	0.0048	17	0.8	1.7	YES
Vigarano ^d	CV3red	1623-9	CTA	1-10	39-570	5.8	1.9	5.8	1.9	0.2422	0.0100	8	1.2	2.1	YES
Efremovka ^f	CV3red	E69	B	5-34		6.1	1.9	6.2	2.0	0.2459	0.0180	12	1.3	1.9	YES
Efremovka ^e	CV3red	E38	B	1-52	14-1677	4.4	0.6	6.5	1.0	0.2503	0.0046	8	0.9	2.1	YES
Leoville ^d	CV3red	3535-3b	CTA	1-14	70-190	6.7	2.4	6.7	2.4	0.2481	0.0126	9	1.7	2.0	YES
Efremovka ^e	CV3red	31E	B	8-79	52-968	4.7	0.8	6.9	1.2	0.2510	0.0026	7	1.0	2.2	YES
Efremovka ⁱ	CV3red	E36	B2			7.0	1.4	7.0	1.1	0.2510	0.0008	20	1.4	1.6	YES
Efremovka ⁱ	CV3red	E65	CTA			7.0	1.7	7.0	1.8	0.2493	0.0014	17	0.8	1.7	YES
Efremovka ^e	CV3red	E48	B	2-90	59-867	4.8	0.3	7.1	0.4	0.2500	0.0020	9	0.9	2.0	YES
Vigarano ^d	CV3red	477-5	FTA	1-20	29-340	7.5	1.9	7.4	1.9	0.2381	0.0138	13	1.6	1.8	YES
Efremovka ^d	CV3red	6456-1	CTA	9-75	300-2160	7.6	1.6	7.6	1.6	0.2520	0.0102	6	1.9	2.3	YES
Efremovka ⁱ	CV3red	E66	B			7.6	2.9	7.6	1.8	0.2498	0.0010	20	2.3	1.6	NO
Efremovka ^f	CV3red	E44	B	10-100		7.6	1.9	7.6	2.4	0.2502	0.0046	13	0.7	1.8	YES
Efremovka ^e	CV3red	E104	CTA	7-66	334-614	5.5	1.4	8.1	2.0	0.2426	0.0062	5	0.5	2.4	YES
Efremovka ^f	CV3red	E48	B	19-96		8.1	3.1	8.2	3.4	0.2490	0.0074	5	0.8	2.4	YES
Efremovka ^e	CV3red	E104	FTA	19-127	165-786	6.7	0.9	9.8	1.3	0.2482	0.0006	8	1.1	2.1	YES
Efremovka ^k	CV3red	E40	B1	4-632	73-536	16.0	10.0	16.0	5.2	0.2347	0.0147	8	3.0	2.1	NO

^a Gounelle *et al.* (2013), ^b Marhas *et al.* (2002), ^c Liu *et al.* (2010), ^d MacPherson *et al.* (2003), ^e Wielandt *et al.* (2012), ^f Sugiura *et al.* (2001), ^g Sossi *et al.* (2017), ^h McKeegan *et al.* (2000), ⁱ Chaussidon (2006), ^j Srinivasen and Chaussidon (2013), ^k Mishra and Marhas (2019).

¹ Mass fractions in ng g⁻¹

^m These $^{10}\text{Be}/^{9}\text{Be}$ ($\times 10^{-4}$) values are those reported in the original publication.

ⁿ These $^{10}\text{Be}/^{9}\text{Be}$ ($\times 10^{-4}$) values were re-calculated based on raw data in the original publication.

^o The is the maximum allowable MSWD for the regression based on the number of data points (n).

^P Validity of isochron regression based on MSWD: YES if $\text{MSWD} < 1 + 2\sigma_{\text{MSWD}}$, NO if $\text{MSWD} > 1 + 2\sigma_{\text{MSWD}}$.

CTA = compact Type-A; FTA = fluffy Type-A; PLAC = platy hibonite; FUN = fractionated and unidentified nuclear effects; hib = hibonite; gros = grossite; px = pyroxene; mel = melilite; sp = spinel.

* The $^{9}\text{Be}/^{11}\text{B}$ values and uncertainties from these studies were estimated because they were not reported, so our regressions are slightly different from the literature values.

We use the example of CAI Lisa, from the Northwest Africa (NWA) 6991 (CV3_{ox}) carbonaceous chondrite, to examine how a regression would change due to irradiation. We used this CAI specifically for this example because its Sm isotope composition suggests that it was irradiated by thermal neutrons (Shollenberger *et al.* 2018). The major element composition of phases in this CAI was determined using the JEOL JXA-8530F EPMA at ASU using conditions similar to those described in section *Elemental compositions*

of melilite-composition glasses. The $^{10}\text{Be}-^{10}\text{B}$ isotope systematics of this CAI were measured with the IMS-1290 SIMS at UCLA using analysis conditions similar to those described earlier (*Analyses with Cameca IMS-1290 SIMS at the University of California, Los Angeles*). These data are reported in Table 4.

From the $^{9}\text{Be}/^{11}\text{B}$ and $^{10}\text{B}/^{11}\text{B}$ ratios of phases in this CAI (Table 4), we calculated an inferred initial

Table 4.
The composition and ^{10}Be – ^{10}B isotope systematics of NWA 6991 (CV3ox) CAI Lisa

CAI SIMS spot	$^9\text{Be}/^{11}\text{B}$	1SE	$^{10}\text{B}/^{11}\text{B}$	1SE	r	[Be] $\mu\text{g g}^{-1}$	[B] $\mu\text{g g}^{-1}$	Al_2O_3 (% m/m)	Ak (mol %)	SiO_2 (% m/m)
Lisa(1290)_1	15.21	0.46	0.2922	0.0110	0.19	0.183	0.018	23	38	27
Lisa(1290)_3	1.72	0.04	0.2481	0.0032	0.20	0.145	0.126	26	28	26
Lisa(1290)_4	17.29	0.55	0.2794	0.0120	0.40	0.250	0.022	24	34	27
Lisa(1290)_5	12.89	0.35	0.2821	0.0070	0.33	0.257	0.030	26	26	25
Lisa(1290)_6	15.27	0.42	0.2756	0.0074	0.35	0.356	0.035	21	43	28
Lisa(1290)_7	6.36	0.16	0.2620	0.0044	0.06	0.349	0.082	24	35	27
Lisa(1290)_8	15.54	0.45	0.2679	0.0086	0.38	0.273	0.026	24	32	26

r is the correlation coefficient.

$^{10}\text{Be}/^9\text{Be} = (2.2 \pm 0.7) \times 10^{-3}$ (MSWD = 1.1). This is much higher (by about 3 times) than in typical CAIs, so we tested whether CAI Lisa could have a high inferred $^{10}\text{Be}/^9\text{Be}$ ratio because its original $^{10}\text{Be}/^9\text{Be}$ ratio was overprinted by an irradiation signature. To do so, we subtracted an assumed spallogenic B contribution ($\Delta[\text{B}]$) from the measured B mass fractions (which ranged from ~ 20 to $\sim 130 \text{ ng g}^{-1}$) and reconstructed the regression. If we can produce a regression with MSWD ~ 1 with a resolvably lower $^{10}\text{Be}/^9\text{Be}$ (say $\sim 7 \times 10^{-4}$, a value similar to most other CAIs; Table 3) by subtracting a reasonable $\Delta[\text{B}]$, then disturbance of the isochron by addition of spallogenic B produced by irradiation of the CAI on the parent body cannot be ruled out.

To determine the original $^9\text{Be}/^{11}\text{B}$ and $^{10}\text{B}/^{11}\text{B}$ ratios before irradiation, we derived and used the following equations:

$$\left(\frac{^9\text{Be}}{^{11}\text{B}}\right)_{\text{original}} = \left(\frac{^9\text{Be}}{^{11}\text{B}}\right)_{\text{measured}} \times \frac{\left[1 - \frac{\Delta[\text{Be}]}{[\text{Be}]}\right]}{\left[1 - \frac{\Delta[\text{B}]}{[\text{B}]} \left(\frac{11.01 + 10.01 \times (^{10}\text{B}/^{11}\text{B})_{\text{measured}}}{11.01 + 10.01 \times 0.44}\right)\right]} \quad (10)$$

$$\left(\frac{^{10}\text{B}}{^{11}\text{B}}\right)_{\text{original}} = \left(\frac{^{10}\text{B}}{^{11}\text{B}}\right)_{\text{measured}} \times \frac{\left[1 - \frac{\Delta[\text{Be}]}{[\text{Be}]} \frac{0.44}{(^{10}\text{B}/^{11}\text{B})_{\text{measured}}} \left(\frac{11.01 + 10.01 \times (^{10}\text{B}/^{11}\text{B})_{\text{measured}}}{11.01 + 10.01 \times 0.44}\right)\right]}{\left[1 - \frac{\Delta[\text{B}]}{[\text{B}]} \left(\frac{11.01 + 10.01 \times (^{10}\text{B}/^{11}\text{B})_{\text{measured}}}{11.01 + 10.01 \times 0.44}\right)\right]} \quad (11)$$

We varied $\Delta[\text{B}]$ and $\Delta[\text{Be}]$, assuming $\Delta[\text{Be}]/\Delta[\text{B}] = 0.1$, then calculated original ratios for each CAI Lisa analysis spot, and constructed a new (pre-irradiation) regression. We found that subtracting only $\sim 2.5 \text{ ng g}^{-1}$ of spallogenic B from each analysis point resulted in a regression consistent at the 2-sigma level with $^{10}\text{Be}/^9\text{Be} \sim 7 \times 10^{-4}$ and with

MSWD ~ 1 (Figure 3). The intercept, that is, the initial $(^{10}\text{B}/^{11}\text{B})_0$, did not change resolvably. In plotting the inferred initial $^{10}\text{Be}/^9\text{Be}$ vs. $\Delta[\text{B}]$ (Figure 4a), we show that as we subtract more hypothetical spallogenic B from the measured abundance, the apparent $^{10}\text{Be}/^9\text{Be}$ decreases systematically. In plotting the inferred initial $^{10}\text{Be}/^9\text{Be}$ vs. MSWD, we show that the MSWD increases slightly as the apparent $^{10}\text{Be}/^9\text{Be}$ decreases, but not drastically enough that the regression could be considered an errorchron (Figure 4b).

When high-energy GCR protons interact with nuclei within the first few metres of the surface of a parent body, a cascade of particle reactions occurs. The cascade produces high-energy neutrons, thermal neutrons (from the deceleration of fast neutrons; Leya *et al.* 2000), protons, and likely some ^{10}Be , ^{10}B and ^{11}B (from protons spalling oxygen nuclei). The isotope ^{149}Sm has a large thermal neutron capture cross section, so it is likely to capture the thermal neutrons (Shollenberger *et al.* 2018). CAI Lisa is measured to have an excess in ^{150}Sm (relative to terrestrial reference materials), the result of neutron capture on ^{149}Sm . This indicates that CAI Lisa experienced an especially high neutron fluence, when compared with other CAIs, of $2.11 \times 10^{15} \text{ n cm}^{-2}$ (Shollenberger *et al.* 2018). This high neutron fluence provides evidence that CAI Lisa was close to the surface of its NWA 6991 parent body, which also had to be bombarded with high-energy cosmic ray protons. We estimate that high-energy proton irradiation of CAIs near the surface of the NWA 6991 parent body can produce ng g^{-1} levels of spallogenic B. We base our findings on Leya *et al.* (2000): irradiation of the uppermost tens of cm of near-surface H chondrite material by the present-day GCR flux at 1 AU can produce the similar isotope ^{10}Be at a rate of seventeen disintegrations per minute per kg. If multiplied by 1 Gy, this would yield a mass fraction of $[^{10}\text{Be}] = 0.15 \text{ ng g}^{-1}$. The cross sections for spallation of ^{16}O to produce the stable isotopes ^{10}B and ^{11}B are, respectively, about 5 and 12 times the cross section for spallation of ^{16}O to produce ^{10}Be (Moskalenko and Mashnik 2003), so we

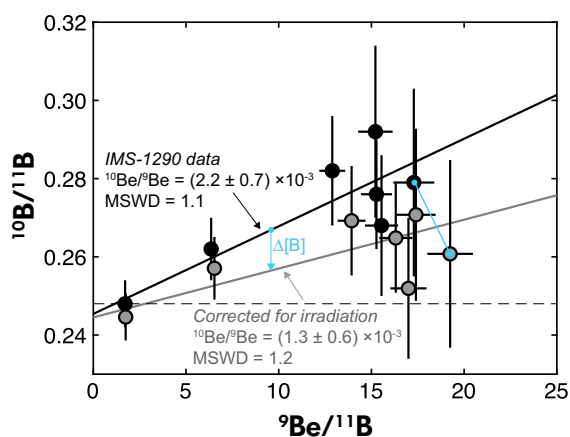


Figure 3. Measured and modelled data for CAI Lisa. The black symbols represent the original IMS-1290 data, and the grey symbols represent the re-calculated regression after subtracting 2.5 ng g^{-1} ($\Delta[B]$) of spallogenic B from the original data. The isochron regression results are shown. The horizontal dashed line is the chondritic B isotope ratio ($^{10}\text{B}/^{11}\text{B} = 0.2481$; Zhai *et al.* 1996). Uncertainties are 2SE.

estimate that irradiation of near-surface chondritic material could raise the mass fraction of boron by 2.8 ng g^{-1} . It is then plausible that high-energy proton irradiation of CAIs near the surface of the NWA 6991 parent body could produce ng g^{-1} levels of spallogenic B necessary to artificially shift the ^{10}Be - ^{10}B systematics of CAI Lisa as illustrated in Figure 3. Future correlated measurements of

^{150}Sm and ^{10}Be in CAIs could verify the possibility that proton irradiation on the surfaces of chondritic parent bodies altered the original ^{10}Be - ^{10}B systematics in some CAIs.

Evidence for aqueous alteration

Another secondary process that could affect the ^{10}Be - ^{10}B system is thermal metamorphism and/or aqueous alteration on the meteorite parent body. We focus on aqueous alteration here because the diffusion coefficients for B in silicates are quite slow (Zhang *et al.* 2010); thermal metamorphism would only cause B to move if a B-bearing phase actually broke down and/or a new boron phase began to grow. Podosek *et al.* (1991) demonstrated that some Allende (CV3_{ox}) CAIs display disturbances in the ^{26}Al - ^{26}Mg system, especially in melilite. Be is refractory and was likely introduced into the CAI at an early stage. It has a 50% condensation temperature of 1500 K as gugiite ($\text{Ca}_2\text{BeSi}_2\text{O}_7$) in solid solution with melilite (Lauretta and Lodders 1997). On the other hand, B has a 50% condensation temperature of only 964 K and was incorporated mostly as danburite (NaBSi_3O_8) in solid solution with anorthite (Lauretta and Lodders 1997). The moderately volatile nature of B causes its depletion in characteristic CAI minerals. Although B diffuses more slowly than Mg (at least in anorthite; Sugiura *et al.* 2001), it may be released to, or precipitated from, an aqueous fluid during parent body alteration.

There are a number of unknowns when discussing the effect of aqueous alteration on the ^{10}Be - ^{10}B regression.

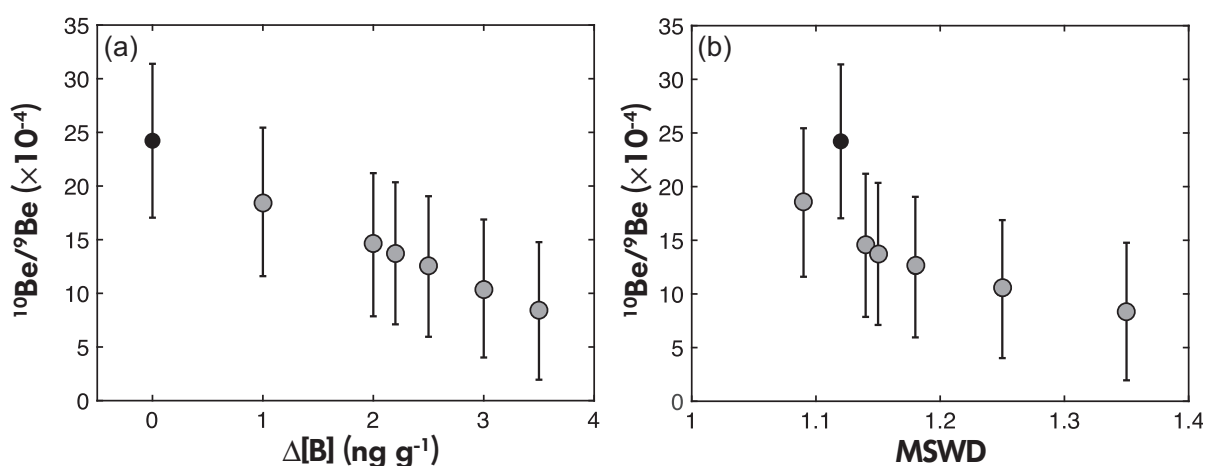


Figure 4. The estimated $^{10}\text{Be}/^9\text{Be}$ ratios based on the measured (black symbol) and modelled (grey symbols) data for CAI Lisa versus (a) the amount of spallogenic B ($\Delta[B]$) subtracted from the total B and (b) MSWD. Panel (a) shows that the inferred initial $^{10}\text{Be}/^9\text{Be}$ ratio decreases as greater amounts of spallogenic B ($\Delta[B]$) are subtracted. Plot (b) shows that the MSWD does not change significantly as more spallogenic B is subtracted, even as the inferred $^{10}\text{Be}/^9\text{Be}$ ratio decreases.

What is the temperature and composition of the aqueous phase? Specifically, what is the B mass fraction and isotopic composition of this phase? What are the diffusion characteristics of B in melilite? It is likely that the fluid-rock interaction is heterogeneous and may only affect a few data points, which would increase the scatter of the data points (adding B to some, subtracting B from others) that define the regression without necessarily altering the inferred initial $^{10}\text{Be}/^9\text{Be}$ ratio. If secondary mineralisation (replacement of melilite by nepheline, sodalite, hedenbergite and andradite; Wasson *et al.* 2001) is present, it proves that alteration by an H_2O -bearing phase occurred. Overall, little information exists about B behaviour during aqueous alteration, especially with regard to melilite, but we expect that any chondritic B exchange between parent body aqueous fluids and melilite would result in more scatter (i.e., higher MSWD) in the CAI ^{10}Be - ^{10}B regression.

Method for future reporting of ^{10}Be - ^{10}B isotope systematics

Integrating the results from future studies of ^{10}Be - ^{10}B isotope systematics in primitive meteoritic materials into a consistently reported data set will increase the scientific impact of this work by allowing comparisons and by enabling an assessment of the original distribution of ^{10}Be in the early Solar System (which has implications for its origin). Comparisons between data sets are only possible if studies follow a standardised reporting procedure. The linear regressions are reproducible only if the authors report these five quantities for each analysis point: $x = ^9\text{Be}/^{11}\text{B}$, uncertainty in x , $y = ^{10}\text{B}/^{11}\text{B}$, and uncertainty in y . The next quantities are also key to report, but are not necessary to reproduce the isochrons: (a) MSWD to assess the robustness of the regression (ideally, authors should also report whether their MSWD exceeds the critical value $1 + 2(2/(n - 2))^{1/2}$, and if so, provide a discussion about the validity of that isochron); (b) the specific reference materials utilised in the study, along with the resulting RSF and IMF values; (c) the compositional data for the phases that are analysed; specifically [B] and [Be] in $\mu\text{g g}^{-1}$ or ng g^{-1} (to enable corrections, as needed, for irradiation), Åk content, abundances of SiO_2 , and Al_2O_3 ; and (d) error correlations (which may not significantly affect the slope of the isochron but can alter the slope uncertainty and MSWD). In following this reporting strategy, researchers will be able to more easily compare results from different studies and interpret the available ^{10}Be - ^{10}B data as a whole.

Conclusions

In the context of determining the origin of ^{10}Be in the early Solar System, we have re-evaluated previous

^{10}Be - ^{10}B studies, while examining the importance of analytical and data reduction factors such as RSF, MSWD, and correlation coefficient, as well as natural factors such as irradiation and aqueous alteration. To properly compare $^{10}\text{Be}/^9\text{Be}$ values between samples to determine whether the distribution of ^{10}Be in the early Solar System was homogeneous or heterogeneous, it is vital to standardise the processing of data obtained via SIMS analyses. Using an inappropriate RSF can change the inferred initial $^{10}\text{Be}/^9\text{Be}$ ratio; we synthesised melilite-composition glass reference materials and agree with Fukuda *et al.* (2018) that matrix-matched reference materials for RSF determination are not necessary to establish accurately determine ^{10}Be - ^{10}B isotope systematics in CAIs. Another measurement consideration to take into account is that individual SIMS analyses should only be made on single-phase, crack-free grains. It is also important to standardise how data are reported. MSWD is essential to report because this quantity allows us to assess the validity of an isochron; specifically, if the MSWD exceeds $1 + 2(2/(n - 2))^{1/2}$, where n is the number of data points in the regression, the regression has < 5% probability of being an isochron (Wendt and Carl 1991). Correlated errors should be taken into consideration when generating a ^{10}Be - ^{10}B isochron because they can affect the uncertainties in the slope and intercept, and the MSWD of a regression. Even after these analytical and data reduction factors are taken into consideration, the inferred initial $^{10}\text{Be}/^9\text{Be}$ ratio may not be the original one in a given CAI. Because B mass fractions in CAI phases are typically low and this element can be produced by proton irradiation, some data sets may need to be corrected for spallogenic B; even a few ng g^{-1} of spallogenic B can change the inferred initial $^{10}\text{Be}/^9\text{Be}$ ratio significantly without affecting the MSWD. Aqueous alteration on the chondrite parent body likely introduces scatter in the ^{10}Be - ^{10}B data and increases the MSWD. The re-evaluated data set presented here (based on data reported previously for thirty-two CAIs), along with implications presented here for the ^{10}Be - ^{10}B isotope system, can be integrated with future studies to constrain the origin of ^{10}Be in the early Solar System.

Acknowledgements

We thank an anonymous reviewer and joint editor-in-chief Dr. Regina Mertz-Kraus for their comments which greatly improved the manuscript. We thank Dr. Kurt Roggensack and Dr. Kurt Leinenweber for helping to develop and implement the melilite glass synthesis procedure. We thank Dr. Steve Romaniello for help with measuring the boron and beryllium mass fractions of the synthetic melilite glasses. We thank Dr. Ming-Chang Liu for helping

with the IMS-1290 measurements as well as for useful discussions. We acknowledge the use of facilities within the Eyring Materials Center at Arizona State University supported in part by NNCI-ECCS-1542160 and the Cameca IMS-6f SIMS laboratory at Arizona State University supported by NSF EAR 1819550. This work was supported by a NASA Earth and Space Science Fellowship (NNX16AP48H) to E.T.D. and a NASA Emerging Worlds grant (NNX15AH41G) to M.W.

Data availability statement

The data that support the findings of this study are available from the corresponding author upon reasonable request.

References

Chaussidon M. (2006)

Li and B isotopic variations in an Allende CAI: Evidence for the *in situ* decay of short-lived ^{10}Be and for the possible presence of the short-lived nuclide ^7Be in the early solar system. *Geochimica et Cosmochimica Acta*, 70, 224–245.

Coath C.D., Steele R.C.J. and Lunnon W.F. (2013)

Statistical bias in isotope ratios. *Journal of Analytical Atomic Spectrometry*, 28, 52–58.

Desch S.J., Connolly H.C. Jr. and Srinivasan G. (2004)

An interstellar origin for the beryllium 10 in calcium-rich, aluminum-rich inclusions. *The Astrophysical Journal*, 602, 528–542.

De Hoog J.C.M., Monteleone B.D., Savov I.P., Marshall H.R. and Zack T. (2017)

Matrix effects in B isotope analysis of silicate minerals by SIMS. *Goldschmidt Conference*.

Dunham E.T., Wadhwa M. and Desch S.J. (2017)

Beryllium-boron systematics of two distinctive CAIs from CV3 chondrites: The relatively pristine CAI B4 from NWA 6991 and the FUN CAI CMS-1 from Allende. (Abstract # 1507), LPSC.

Fukuda K., Fujiya W., Hiyagon H., Makino Y., Sugiura N., Takahata N., Hirata T. and Sano Y. (2018)

Beryllium-boron relative sensitivity factors for melilitic glasses measured with a NanoSIMS ion microprobe. *Geochemical Journal*, 52, 1–8.

Gangjian W., Jingxian W., Ying L., Ting K., Zhongyuan R., Jinlong M. and Yigang X. (2013)

Measurement on high-precision boron isotope of silicate materials by a single column purification method and MC-ICP-MS. *Journal of Analytical Atomic Spectrometry*, 28, 606–612.

Gnaser H. and Hutcheon I.D. (1987)

Velocity-dependent isotope fractionation in secondary ion emission. *Physical Review*, B, 35, 877–879.

Gounelle M., Shu F.H., Shang H., Glassgold A.E., Rehm K.E. and Lee T. (2001)

Extinct radioactivities and protosolar cosmic rays: Self-shielding and light elements. *The Astrophysical Journal*, 548, 1051–1070.

Gounelle M., Chaussidon M. and Rollion-Bard C. (2013)

Variable and extreme irradiation conditions in the early solar system inferred from the initial abundance of ^{10}Be in Isheyevo CAIs. *The Astrophysical Journal*, 763, L33.

Hervig R.L., Mazdab F.K., Williams P., Guan Y., Huss G.R. and Leshin L.A. (2006)

Useful ion yields for Cameca IMS 3f and 6f SIMS: Limits on quantitative analysis. *Chemical Geology*, 227, 83–99.

Ihinger P.D., Hervig R.L. and McMillan P.M. (1994)

Analytical methods for volatiles in glasses. In: Carroll M.R. and Holloway J.R. (eds), *Reviews in Mineralogy: Volatiles in Magmas*. De Gruyter Mouton (Berlin), 67–121.

Jacquet E. (2019)

On beryllium-10 production in gaseous protoplanetary disks and implications on the astrophysical setting of refractory inclusions. *Astronomy and Astrophysics*, 624, A131.

Jochum K.P., Willbold M., Raczek I., Stoll B. and Herwig K. (2005)

Chemical characterisation of the USGS reference glasses GSA-1G, GSC-1G, GSD-1G, GSE-1G, BCR-2G, BHVO-2G and BIR-1G using EPMA, ID-TIMS, ID-ICP-MS and LA-ICP-MS. *Geostandards and Geoanalytical Research*, 29, 285–302.

Jochum K.P., Weis U., Stoll B., Kuzmin D., Yang Q., Raczek I., Jacob D.E., Stracke A., Birbaum K., Frick D.A., Günther D. and Enzweiler J. (2011)

Determination of reference values for NIST SRM 610–617 glasses following ISO guidelines. *Geostandards and Geoanalytical Research*, 35, 397–429.

Korschinek G., Bergmaier A., Faestermann T., Gerstmann U., Knie K., Rugel G., Wallner A., Dillmann I., Dollinger G., von Gostomski C.L., Kossert K., Maiti M., Poutivtsev M. and Remmert A. (2010)

A new value for the half-life of ^{10}Be by heavy-ion elastic recoil detection and liquid scintillation counting. *Nuclear Instruments and Methods in Physics Research, Section B*, 268, 187–191.

Lauretta D.S. and Lodders K. (1997)

The cosmochemical behavior of beryllium and boron. *Earth and Planetary Science Letters*, 146, 315–327.

Leya I., Lange H.J., Neumann S., Wieler R. and Michel R. (2000)

The production of cosmogenic nuclides in stony meteoroids by galactic cosmic-ray particles. *Meteoritics and Planetary Science*, 35, 259–286.

Liu M.-C., Nittler L.R., Alexander C.M.O. and Lee T. (2010)

Be and early solar system irradiation. *The Astrophysical Journal*, 719, L99–L103.

references

Liu M.-C., McKeegan K.D., Harrison T.M. and Jarzabinski G. (2018)

The Hyperion-II radio-frequency oxygen ion source on the UCLA ims 1290 ion microprobe: Beam characterization and applications in geochemistry and cosmochemistry. *International Journal of Mass Spectrometry*, 424, 1–9.

Ludwig K.R. (1988)

Isoplot for MS-DOS: A plotting and regression program for radiogenic-isotope data, for IBM-PC compatible computers. *United States Geological Survey*, 88–557, 1–37.

MacPherson G.J., Huss G.R. and Davis A.M. (2003)

Extinct ^{10}Be in Type A calcium-aluminum-rich inclusions from CV chondrites. *Geochimica et Cosmochimica Acta*, 67, 3165–3179.

Marhas K.K., Goswami J.N. and Davis A.M. (2002)

Short-lived nuclides in hibonite grains from Murchison: Evidence for solar system evolution. *Science*, 298, 2182–2185.

Marschall H.R. and Monteleone B.D. (2014)

Boron isotope analysis of silicate glass with very low boron concentrations by secondary ion mass spectrometry. *Geostandards and Geoanalytical Research*, 39, 31–46.

McKeegan K.D., Chaussidon M. and Robert F. (2000)

Incorporation of short-lived ^{10}Be in a calcium-aluminum-rich inclusion from the Allende meteorite. *Science*, 289, 1334–1337.

Mishra R.K. and Marhas K.K. (2019)

Meteoritic evidence of a late superflare as source of ^7Be in the early Solar System. *Nature Astronomy*, 3, 498–505.

Moskalenko I.V. and Mashnik S.G. (2003)

Evaluation of production cross sections of Li, Be, B in CR. The 28th International Cosmic Ray Conference, 1–14.

Ogliore R.C., Huss G.R. and Nagashima K. (2011)

Ratio estimation in SIMS analysis. Nuclear instruments and methods in physics research section B: beam interactions with materials and atoms, 269, 1910–1918.

Ottolini L., Camara F., Hawthorne F.C. and Stirling J. (2002)

SIMS matrix effects in the analysis of light elements in silicate minerals: Comparison with SREF and EPMA data. *American Mineralogist*, 87, 1477–1485.

Podosek F.A., Zinner E.K., MacPherson G.J., Lundberg L.L., Brannon J.C. and Fahey A.J. (1991)

Correlated study of initial $^{87}\text{Sr}/^{86}\text{Sr}$ and Al/Mg isotopic systematics and petrologic properties in a suite of refractory inclusions from the Allende meteorite. *Geochimica et Cosmochimica Acta*, 55, 1083–1110.

Rosner M., Wiedenbeck M. and Ludwig T. (2008)

Composition-induced variation in SIMS IMF during boron isotope ratio measurements of silicate glasses. *Geostandards and Geoanalytical Research*, 32, 27–38.

Shollenberger Q.R., Borg L.E., Render J., Ebert S., Bischoff A., Russell S.S. and Brennecka G.A. (2018)

Isotopic coherence of refractory inclusions from CV and CK meteorites: Evidence from multiple isotope systems. *Geochimica et Cosmochimica Acta*, 228, 62–80.

Sossi P.A., Moynier F., Chaussidon M., Villeneuve J., Kato C. and Gounelle M. (2017)

Early Solar System irradiation quantified by linked vanadium and beryllium isotope variations in meteorites. *Nature Astronomy*, 1, 0055.

Srinivasan G. and Chaussidon M. (2013)

Constraints on ^{10}Be and ^{41}Ca distribution in the early solar system from ^{26}Al and ^{10}Be studies of Efremovka CAIs. *Earth and Planetary Science Letters*, 374, 11–23.

Sugiura N., Shuzou Y. and Ulyanov A. (2001)

Beryllium-boron and aluminum-magnesium chronology of calcium-aluminum-rich inclusions in CV chondrites. *Meteoritics and Planetary Science*, 1408, 1397–1408.

Tatischeff V., Duprat J. and De Sereville N. (2014)

Light-element nucleosynthesis in a molecular cloud interacting with a supernova remnant and the origin of beryllium-10 in the protosolar nebula. *The Astrophysical Journal*, 796, 124–144.

Telus M., Huss G.R., Ogliore R.C., Nagashima K. and Tachibana S. (2013)

Recalculation of data for short-lived radionuclide systems using less-biased ratio estimation. *Meteoritics and Planetary Science*, 2030, 2013–2030.

Vermeech P. (2018)

IsoplotR: A free and open toolbox for geochronology. *Geoscience Frontiers*, 9, 1479–1493.

Wasson J.T., Yurimoto H. and Russell S.S. (2001)

^{16}O -rich melilite in CO3.0 chondrites: Possible formation of common, ^{16}O -poor melilite by aqueous alteration. *Geochimica et Cosmochimica Acta*, 65, 4539–4549.

Wendt I. and Carl C. (1991)

The statistical distribution of the mean squared weighted deviation. *Chemical Geology (Isotope Geoscience Section)*, 86, 275–285.

Wielandt D., Nagashima K., Krot A.N., Huss G.R., Ivanova M.A. and Bizzarro M. (2012)

Be in the early Solar System. *The Astrophysical Journal*, 748, L25.

York D. (1966)

Least-squares fitting of a straight line. *Canadian Journal of Physics*, 44, 1079–1086.

York D., Evensen N.M., Martínez M.L. and De Basabe Delgado J. (2004)

Unified equations for the slope, intercept, and standard errors of the best straight line. *American Journal of Physics*, 72, 367–375.



references

Zhai M., Nakamura E., Shaw D.M. and Nakano T.
(1996)
Boron isotope ratios in meteorites and lunar rocks.
Geochimica et cosmochimica acta, 60, 4877–4881.

Zhang Y., Ni H. and Chen Y. (2010)
Diffusion data in silicate melts. *Reviews in Mineralogy and
Geochemistry*, 72, 311–408.